Published in final edited form as:
Mol Ther. 2010 February ; 18(2): 285. doi:10.1038/mt.2009.232.

Enhanced anti tumor efficacy of Vasculostatin (Vstat120) expressing oncolytic HSV-1

Jayson Hardcastle[1,2,5], **Kazuhiko Kurozumi**[1,5,8], **Nina Dmitrieva**[1,5], **Martin P Sayers**[1,3,5], **Sarwat Ahmad**[4,5], **Peter Waterman**[6,7], **Ralph Weissleder**[6,7], **E Antonio Chiocca**[1,5], and **Balveen Kaur**[1,5,*]

[1]Dardinger Laboratory for Neuro-oncology and Neurosciences, The Ohio State university Medical center, Columbus, OH., 43210

[2]Integrated Biomedical Sciences, Graduate Program, The Ohio State university Medical center, Columbus, OH., 43210

[3]Undergraduate Major in Biomedical Science, The Ohio State university Medical center, Columbus, OH., 43210

[4]College of Medicine, The Ohio State university Medical center, Columbus, OH., 43210

[5]Department of Neurological Surgery, *James Comprehensive Cancer Center* and The Ohio State university Medical center, Columbus, OH., 43210

[6]Center for Molecular Imaging Research, Massachusetts General Hospital, Charlestown, MA., 02129 USA

[7]Center for Systems Biology, Massachusetts General Boston, MA02114

Abstract

Oncolytic viral therapy is a promising therapeutic modality for brain tumors. Vasculostatin (Vstat120), is the cleaved and secreted extracellular fragment of BAI1, a brain specific receptor. However, the therapeutic efficacy of Vstat120 delivery into established tumors has not been investigated. Here we tested therapeutic efficacy of combining Vstat120 gene delivery in conjunction with oncolytic viral therapy. We constructed a novel oncolytic virus RAMBO: **R**apid **A**nti-angiogensis **M**ediated **B**y **O**ncolytic virus, which expresses Vsta120 under the control of an immediate early viral promotor. Secreted Vstat120 was detectable in infected cells as soon as four hours post infection. Vstat120 produced by RAMBO efficiently inhibited endothelial cell migration and tube formation in vitro (P=0.0005 and P=0.0184 respectively) and inhibited angiogeneisis (P=0.007) *in vivo*. There was a significant suppression of tumors growth in mice bearing intracranial and subcutaneous gliomas treated with RAMBO compared to the control HSVQ treated mice (P=0.0021, and P<0.05 respectively). Statistically significant reduction in tumor vascular volume fraction and microvessel density was observed in tumors treated with RAMBO. This study is the first report of antitumor effects of Vstat120 in established tumors and supports the further development of RAMBO as a possible treatment for cancer.

*Correspondence should be addressed to: Balveen Kaur, Department of Neurological Surgery, Dardinger Laboratory for Neuro-oncology and Neurosciences, The Ohio State University, 385-D OSUCCC, 410 West 12th Avenue, Columbus, OH 43210. Balveen.Kaur@osumc.edu, Phone: 614 292 3984, fax: 614 688 4882.
[8]Current Address: Department of Neurological Surgery, Okayama University Graduate School of Medicine, Okayama, Japan.

Keywords

Glioma; Vasculostatin; Oncolytic virus; HSV-1; angiogenesis

INTRODUCTION

Glioblastoma multiforme (GBM), is the most common and malignant form of brain tumors and even after decades of research the median survival of patients treated with radiation and chemotherapy remains less than fifteen months[1]. Despite the molecular heterogeneity of genetic alterations observed in malignant gliomas, increased vascularity and micro-vascular proliferation remains one of its histopathologic hallmarks. The concept of using antiangiogenic strategies to block tumor vasculature as a therapeutic strategy for glioma is currently being tested in human patients[2]. While these studies have yielded encouraging results, it is becoming increasingly obvious that a multipronged therapeutic approach combining antiangiogenic agents with cytotoxic agents will be essential to combat this deadly disease.

Another promising new direction in cancer therapy is the use of oncolytic viruses (OV), which exploit tumor specific conditions to infect and/or replicate in cancer cells leading to their oncolytic destruction[3]. PhaseI/II clinical testing of OV has demonstrated the relative safety of this approach in human patients up to doses of 10^9 pfu with no therapy associated toxicity or adverse events[4,5]. Future large randomized phase III clinical trials will evaluate therapeutic efficacy of this approach.

One of the major limitations in OV therapy is the rapid innate immune responses initiated in tumors upon infection. This antiviral immune response is accompanied by the secretion of several pro-angiogenic factors[6–11] which can induce angiogenesis and encourage growth of residual tumor after viral clearance. Corneal infection of wild type HSV-1 has also been, linked to increased expression of angiogenic factors, such as VEGF, MMP9, Cox-2, and reduced expression of antiangiogenic factors, such as TSP-1 and TSP-2[11,12]. Consistent with these studies we and others have recently reported a significant increase in cysteine rich 61 (cyr61), and reduction of antiangiogenic thrombospondin 1 (TSP-1) after oncolytic HSV-1 treatment [11,12]. Cyr61 mediated $\alpha_v\beta_5$ [13] integrin activation and reduced TSP-1 (antiangiogenic ligand for CD36 on ndothelial cells) levels have been implicated in increased angiogenesis of the residual tumor that regrows following OV mediated tumor destruction and viral clearance [14].

Vasculostatin (Vstat120) is the extracellular fragment of Brain Specific Angiogenesis Inhibitor 1 (BAI1), and has been shown to be a potent antiangiogenic and antitumorigenic factor. Vstat120 contains five TSP type 1 repeats (amino acids 264–315; 357–407; 412–462; 470–520; and 525–575) and an integrin antagonizing RGD motif (amino acids 231–233)[15]. Both the TSRs as well as the RGD integrin-binding domains of BAI1 have been shown to have antiangiogenic functions[16,17]. The RGD integrin binding motif of BAI1 has been shown to be angiostatic by antagonizing activation of $\alpha_v\beta_5$ family of integrins[18]. The five TSP1 domains of Vstat120 have also been shown to be antiangiogenic *in vitro* and *in vivo*[19,20]. While armed oncolytic HSV-1 derived viruses expressing a variety of angiostatic factors have been described[21–25], we hypothesized that efficient production of Vstat120 expressed under the IE4/5 HSV promotor would counter the reduction of TSP-1 and increased CYR61 integrin activation in the glioma microenvironment thereby leading to enhanced anti-glioma efficacy of OV (Figure 1).

We have created an armed oncolytic HSV-1 that expresses Vstat120 under the expression of an immediate early IE4/5 HSV promoter. Based on the potent and rapid induction of

antiangiogenic Vstat120 we named this virus RAMBO (**R**apid **Anti**angiogensis **M**ediated **B**y **O**ncolytic virus). Treatment of mice bearing intracranial and subcutaneous gliomas revealed a significant increase in anti-tumor efficacy of RAMBO compared to the control HSVQ virus. This is the first study to investigate therapeutic efficacy of Vstat120 delivery in established tumors.

RESULTS

Engineering of RAMBO (Rapid Antiangiogensis Mediated By Oncolytic virus)

To test the efficacy of Vstat120 gene delivery by OV, we created RAMBO, an oncolytic HSV-1 expressing Vstat120. The engineering strategy for RAMBO was to incorporate the cDNA encoding for human Vstat120, driven by the HSV-1 IE4/5 promoter, within the backbone of an attenuated HSV-1 virus (HSVQ). HSVQ is deleted for both the copies of γ34.5 genes and a gene disrupting insertion of GFP within the viral UL39 locus encoding for ICP6 gene (Supplementary Fig. S.1, **available online**). We employed the HSVQuik technology to create RAMBO (detailed in materials and methods section)[26]. Correct insertion of the Vstat120 expression cassette into the isolated RAMBO-BAC was confirmed by XhoI restriction digest (Fig. 2a), and PCR amplification (Fig. 2b). The selected RAMBO-BAC was then used to generate the infectious recombinant RAMBO virus [20]. Southern blot analysis of XhoI digested HSVQ and RAMBO was used to confirm the correct recombinant virus (Fig. 2c).

In vitro and *in vivo* production of Vstat120 by RAMBO

Next we tested the temporal pattern of expression of Vstat120 in glioma cells infected with RAMBO *in vitro* and *in vivo*. Cell lysates, and secreted extracellular matrix (ECMs) of LN229 cells infected with HSVQ or RAMBO were harvested at the indicated time points and the expression of Vstat120 was probed by western blot analysis (Fig. 2d). Vstat120 was detected in cell lysate and secreted ECM as soon as four hours post RAMBO infection of cells *in vitro*. To confirm production of Vstat120 *in vivo*, mice with established subcutaneous tumors (U87ΔEGFR-Luc) were treated with a single dose of 8×10^5 pfu of RAMBO by direct intratumoral injection. The mice were sacrificed at the indicated time points following injection and the harvested tumors were analyzed for Vstat120 expression by Western blot analysis (Fig. 2e). Vstat120 expression could be detected in tumors treated with RAMBO for 13 days post OV therapy. Collectively these results indicated efficient *in vitro* and *in vivo* production of Vstat120 that persists for a lengthy time upon infection with single dose of RAMBO. Western blot analysis of RAMBO treated intracranial tumors in mice confirmed Vstat120 expression by RAMBO but not HSVQ in vivo (Supplementary Fig. S.2, **available on line**).

RAMBO replicates efficiently and is cytotoxic to glioma cells in vitro

We compared the *in vitro* cytotoxicity of a panel of glioma cell lines infected with RAMBO to HSVQ. Four established human glioma cell lines (LN229, U87ΔEGFR, Gli36ΔEGFR-H2B-RFP and U343) were treated with HSVQ or RAMBO at 0, 0.05, 0.1, 0.5, or 1 MOI. Three days post infection cell viability was assessed (Fig. 3a). No statistically significant difference between RAMBO and HSVQ mediated cytotoxicity was apparent for any of the tested glioma cell lines. Next we compared the replication of RAMBO to HSVQ in glioma cells by a virus yield assay. Glioma cell lines (LN229, U343, and U87ΔEGFR) were infected with RAMBO or HSVQ and 72 hrs after infection the number of infectious viral particles (pfu) produced in each cell line was assessed. Supplementary-Table 1 (available on line) shows the results of viral titration in each indicated cell line. Collectively these results indicate that RAMBO could efficiently infect/replicate in glioma cells *in vitro*.

We next compared the cytotoxicity of RAMBO and HSVQ towards normal human astrocytes (NHA) in culture. NHA cells were infected with RAMBO or HSVQ at the indicated MOIs.

Three days later, cytotoxicity was measured by crystal violet assay. Fig. 3b shows no significant difference in the number of viable cells at all tested MOIs between RAMBO and HSVQ infected NHA cells. G207, is an oncolytic HSV-1 derived virus with similar mutations as HSVQ. This virus has been tested in HSV-1 susceptible mice and non human primates and was found to be safe when injected intracerebrally or intraventricularly up to doses as high as 10^7 (mice) and 10^9 (monkeys)[27,28]. Further clinical testing of G207 has revealed no apparent toxicity with injections of G207 directly into intracranial tumors or after resection into the adjacent brain [29]. However detailed toxicity and biodistribution studies would need to be carried out prior to the clinical evaluation of RAMBO for safety and efficacy in human patients.

RAMBO, exhibits potent antiangiogenic effects *in vitro* and *in vivo*

Vstat120 has been shown to exert its antiangiogenic effects against both human and mouse endothelial cells in vitro and in vivo [20]. To evaluate the functionality of Vstat120 produced by RAMBO we tested if conditioned medium (CM) from glioma cells infected with RAMBO inhibited cell migration and tube formation of Human dermal microvascular endothelial (HDMEC) cells as previously described [15]. HDMECs pretreated with (CM) derived from PBS, HSVQ, or RAMBO treated U251T2 cells, (verification of Vstat120 CM Supplementary Fig. S.3, available online) were assessed for their ability to form tubes on matrigel coated plates. The number of tubes formed in the center of each well (n=4/group) was quantified. Fig. 4A shows a significant reduction in the number of tubes formed by endothelial cells treated with CM from RAMBO infected cells compared to those made by PBS or HSVQ treated cells (P=0.027 and P=0.018 respectively). The bottom panel shows representative pictures of tubes formed by endothelial cells treated with PBS, HSVQ, and RAMBO CM.

HDMECs treated with CM from PBS, HSVQ, or RAMBO infected U251T2 glioma cells, were compared for their ability to migrate in a transwell assay. The cells were plated in the upper portion of the transwell chambers and allowed to migrate towards complete HDMEC media used as a chemo-attractant in the bottom chamber. The migrated cells on the bottom side of the filter were visualized and quantified. Fig. 4B shows a statistically significant reduction in the migration of endothelial cells treated with CM derived from RAMBO infected cells compared to PBS and HSVQ treated cells (P=0.0004 and P=0.0005 respectively).

Next we tested the angiostatic effect of RAMBO treatment *in vivo* using a Directed *In Vivo* Angiogenesis Assay (DIVAA) as described in materials and methods. Quantification of the amount of hemoglobin in each angioreactor, revealed a statistically significant reduction in angiogenesis in RAMBO treated angioreactors compared to PBS and HSVQ (P=0.0022, and 0.007 respectively)(Fig. 4C). The bottom panel shows representative images of angioreactors at the time of harvest. Visually the amount of angiogenesis initiated into the tubes through the one open end was greatly reduced in RAMBO treated angioreactors compared to the PBS and HSVQ samples. These results indicate the potent *in vitro* and *in vivo* angiostatic effect of RAMBO compared to HSVQ.

RAMBO has improved antitumor efficacy against *in vivo* subcutaneous and intracranial gliomas

We first tested the antitumor efficacy of RAMBO against subcutaneous Gli36ΔEGFR – H2B-RFP glioma tumors in athymic nude mice. Mice with subcutaneous tumors (150–250 mm^3) were treated with PBS, HSVQ, or RAMBO, and then were closely monitored for tumor growth. Fig. 5A shows the tumor growth of individual mice from PBS (top panel), HSVQ (middle panel) and RAMBO (bottom panel) treated groups. All mice treated with PBS rapidly progressed after treatment. There was a trend towards enhanced survival in mice treated with HSVQ compared to PBS treatment. One out of the six HSVQ treated mice appeared to have had stable disease until day 22 after which it rapidly progressed. Half of the RAMBO treated

mice showed a complete response and one out of the six mice had a stable disease up to day 25, and then progressed. Fig. 5B shows Kaplan-Meier survival curve of mice treated with PBS, HSVQ, or RAMBO. There was a statistically significant increase in survival of mice (n=6/group) treated with RAMBO compared to HSVQ (median survival=62.5 and 16.5 days respectively) (P=0.038).

Next we compared the antitumor efficacy of RAMBO to HSVQ in mice bearing intracranial glioma (U78ΔEGFR). Seven days post tumor implantation the mice were treated with a single dose of PBS, HSVQ, or RAMBO by direct intratumoral injection. The survival of mice in each group (n =5/group) was analyzed by Kaplan-Meier curve (Fig. 5C). Control mice treated with PBS died of tumor burden with a median survival of 20 days. Mice treated with RAMBO had more than a doubling of the median survival compared to HSVQ treated mice (median survival = 54 and 26 days respectively) (P=0.002). One out of the 5 RAMBO treated mice survived more than 120 days at which time the mouse was sacrificed and was found to be tumor free by histologic examination. Conversely, all HSVQ treated mice had to be sacrificed by day 27 due to tumor burden (tumor confirmed by gross histology).

In a separate experiment mice with intracranial gliomas (U78ΔEGFR) treated with HSVQ or RAMBO were sacrificed on days 1, 2, 3, 8, 13, 18, 23, 32 post viral therapy and the brains preserved for immunohistochemistry and histolopathogical analysis. Histopathological analysis of high resolution scans of the cryosectioned mouse brains revealed equal regression of the gliomas (arrows) following treatment with either RAMBO or HSVQ (Fig. 5D). Regrowth of the residual tumor became evident, in HSVQ treated mice thirteen days post OV treatment (day 20), and two of the 3 mice sacrificed at this time point had significantly large tumors and were symptomatic of tumor burden, while none of the RAMBO treated mice showed regrowth of the residual disease until 39 days post OV therapy. This suggested that RAMBO treatment of intracranial tumors was able to suppress the regrowth of residual tumor after oncolysis compared to HSVQ treated mice.

Changes in microvessel density and vascular volume fraction in established tumors treated with RAMBO

To determine if RAMBO therapy of tumors resulted in impaired vascular supply recruitment needed for tumor regrowth, we compared the microvessel density (MVD) and vascular volume fraction (VVF) of tumors treated with HSVQ or RAMBO. Six days after subcutaneous glioma cell implantation (U87ΔEGFR-Luc) the mice were treated with a single intratumoral injection of PBS, HSVQ, or RAMBO. Twelve days post OV therapy tumors were harvested and sections were stained for CD31, a vascular marker, to visualize vessels (Fig. 6A). Enumeration of the microvessels revealed a statistically significant reduction in MVD for tumors treated with RAMBO compared to HSVQ and PBS (P=0.0001, and 0.0001 respectively) (Fig. 6B).

In a separate experiment the changes in VVF were assessed by fluorescence molecular tomography (FMT) in live animals (Fig. 6c–d). Fig. 6C shows representative FMT images of mice treated with PBS, HSVQ or RAMBO. Mice bearing subcutaneous U87ΔEGFR-Luc tumors were treated as described above then injected with a vascular marker, AngioSense680, and underwent FMT imaging a day prior to OV injection (Fig. 6c, left panel) and then twelve days post OV injection (Fig. 6c, right panel). Local fluorescence concentrations were color coded. A shift towards red indicates a higher fluorochrome concentration and a shift towards blue indicates lower fluorochrome concentration. Higher fluorochrome concentration indicates higher vascular perfusion in that area. Relative vascular volume fractions (VVF) were calculated by dividing the total fluorochrome concentration in each tumor with the corresponding tumor volume. Fig. 6d shows the change in VVF in each mice treated by PBS, HSVQ or RAMBO. VVF change is calculated by subtracting the pre-therapy VVF for each mice from the post therapy VVF. The aggressive growth of PBS treated tumors resulted in

larger tumors that had areas of necrosis and poor vascularity (0–38nM fluorochrome concentrations) along with some areas of very high perfusion (113–150nM fluorochrome concentrations). Thus tumor size normalized VVF change for PBS treated tumors had a trend to be lower than that for HSVQ and RAMBO. Between the relatively similar sized HSVQ and RAMBO tumors, HSVQ had better perfusion (0–75nM fluorochrome concentration) than RAMBO, (0–38nM fluorochrome concentrations). There was a statistically significant reduction in VVF change in tumors of mice treated with RAMBO relative to HSVQ treated tumors ($P<0.05$).

DISCUSSION

Development of tumor vasculature is a critical step during tumor progression, and is critical for the growth and progression of solid tumors. BAI1 has been shown to have angiostatic effects and is absent in approximately 72% of the human GBM specimens tested while the surrounding non-neoplastic tissue retains BAI1 expression [30]. This suggests the possibility that the loss of this protein imparts a growth advantage to the tumor aiding in its vascular development. Here we report the preclinical efficacy of RAMBO: a novel HSV-1 derived OV expressing antiangiogenic Vstat120 under the control of an immediate early viral promoter. This is the first study investigating the potential of Vstat120 gene delivery as a therapeutic modality in established tumors *in vivo*. Our results indicate that Vstat120 produced by RAMBO is functional and does not interfere with tumor cell oncolysis. Treatment of subcutaneous and intracranial gliomas with RAMBO revealed efficient antitumor and antiangiogenic effects compared to control HSVQ. Immunohistochemistry and FMT analysis of mouse xenografts treated with RAMBO revealed a significant reduction in MVD and VVF.

OV treatment of experimental rat gliomas, has been shown to result in vascular hyper-permeability, in the tumor [31]. The increased vascular leakage in OV–treated gliomas was associated with tumor tissue inflammation and CD45–positive leukocyte infiltration, which has been associated with increased viral clearance [32–34]. The key role played by blood vessels in facilitating tissue inflammation is bolstered by the observation that increased MVD in transgenic mice engineered to over express vascular endothelial growth factor A (VEGF-A) or placental growth factor (PLGF) results in an exaggerated and prolonged inflammatory response [35,36]. Together, these studies emphasize the key role played by increased vessel density in facilitating tissue inflammation. The increased microvessel density characteristic of solid tumors may aggravate antiviral host responses leading to rapid viral clearance and reduced antitumor efficacy.

Consistent with these observations, we have shown that reduction of tumoral blood vessel density by a single dose of angiostatic cRGD peptide treatment prior to oncolytic HSV-1 treatment reduced OV induced hyperpermability and tumor inflammation and prolonged tumoral viral propagation hence enhancing antitumor efficacy of OV [32]. This observation is strengthened by a recent observation that treatment of tumors with bevacizumab (anti-VEGF monoclonal antibody) was also shown to improve spread and anti tumor efficacy of oncolytic Adenovirus *in vivo*[37]. Here we show that RAMBO, an armed OV expressing Vstat120, had a significantly greater anti tumor effect compared to the OV treatment alone. RAMBO treated tumors also showed a significant reduction in tumor MVD and VVF. While the increase in antitumor efficacy of RAMBO may be attributed to its ability to counter OV induced angiogenic changes in the tumor microenvironment, future studies will elucidate if Vstat120 expression also affects intratumoral OV propagation and antiviral immune responses in the tumor.

Vstat120 is the extracellular portion of BAI1 which is secreted as a result of proteolytic processing at a conserved G protein coupled receptor proteolytic cleavage site (GPS) [26].

BAI1 is a seven transmembrane receptor expressed primarily in normal brain but absent in a majority of primary GBM, glioma cell lines, and metastatic brain cancers [19,30,38–40]. Reduced expression of BAI1 has also been noted in a variety of other malignancies, including pulmonary adenocarcinoma, pancreatic and gastric cancers[41–44] suggesting that its loss may confer a growth advantage and restoration of its expression may have a therapeutic effect. In agreement with this, stable over-expression of human BAI1 and Vstat120 in glioma cells has been shown to suppress the growth of multiple subcutaneous and intracranial tumors [15,44]. Suppression of the tumor growth, even in the presence of the strong pro-oncogene Epidermal Growth Factor Receptor variant III (EGFRvIII), may have been through Vstat120's ability to bind to CD36 via its TSP-1 repeats or through integrin binding via its RGD motif to $\alpha_v\beta_5$ on endothelial cells[18,20],, More recently BAI1 has been shown to function as an engulfment receptor on macrophages [45]. Future studies will elucidate if Vstat120 also plays a role in macrophage engulfment and how this may contribute towards its therapeutic efficacy *in vivo*.

In conclusion, this study underscores the significance of combining angiostatic strategies with oncolytic virus therapy. This is the first study describing the therapeutic efficacy of Vstat120 gene delivery in established tumors and future work with this virus could lead to a new therapeutic modality to combat cancer.

MATERIALS AND METHODS

Cells and Viruses

U343, U87, U87ΔEGFR, LN229, Gli36ΔEGFR-H2B-RFP, U251-T2, U87ΔEGFR-Luc, human glioma cells and Vero cells were maintained as described[46]. Normal human astrocytes (NHA) and human dermal microvascular endothelial cells (HDMECs) were purchased from Sciencell, (Carlesbad, CA; cat#1800). U87ΔEGFR and U87ΔEGFR-Luc cells lines express a truncated, constitutively active, mutant form of epidermal growth factor receptor (EGFRvIII) and U87ΔEGFR-Luc cells constitutively express luciferase as well. Gli36ΔEGFR-H2B-RFP cells also express the EGFRvIII receptor and has a histone-2B-RFP[26,47]. RAMBO was generated as previously described[26].

Cytotoxicity assays

Cytotoxicityy of RAMBO, and HSVQ was assessed by crystal violet assay[30]. Indicated cell lines were infected at the indicated multiplicity of infection (MOI), and at the days indicated the cells were fixed with 1% glutaraldehyde, and stained with 0.5% crystal violet. After washing, the crystals were dissolved in Sorenson's buffer (0.025M sodium citrate, 0.025M citric acid in 50% ethanol) and absorbance read at A_{590} nm.

Western blot analysis

Immunoblots were performed on cell lysates, conditioned medium (CM) or extra-cellular-matrix (ECM) as previously described[46]. Immunoblots were probed with rabbit anti-N-terminal BAI1[48], or anti-human GAPDH (Abcam, Cambridge, Ma), anti-ICP4 (Abcam, Cambridge, Ma), or anti-gC (Abcam, Cambridge, MA) antibodies, followed by goat anti-rabbit (DAKO Co. Carpinteria CA) or sheep anti-mouse (Amersham Biosciences, Pitsburg, PA) secondary antibodies, and visualized by enhanced chemiluminescence (GE HealthCare, Pitsburg, PA).

Animal Surgery

All animal experiments were performed according to the Subcommittee on Research Animal Care of the Ohio State University guidelines and have been approved by the Institutional Review Board. 6–8 week old athymic nude mice, (Charles River Laboratories, Inc., Frederick,

MD) were used for all studies. **D**irected **I**n **V**ivo Antiangiogenesis **A**ssay (DIVAA) was performed as per manufacturer's instructions (Trevigen, Gaithersburg, MD). Briefly angioreactors filled with growth factor reduced BME containing (2.5×10^5) U87ΔEGFR glioma cells treated with PBS or (1.875×10^4 pfu) of HSVQ or RAMBO and were implanted subcutaneously in mice for eleven days. Angioreactors were excised out and hemoglobin content was quantified by a standard hemoglobin assay (Wako Diagnostics, Richmond, VA).

For intracranial-tumor studies, anesthetized mice were fixed in a stereotactic apparatus and a burr hole was drilled at 2 mm lateral to the bregma, to a depth of 3 mm. Seven days after tumor cell implantation of U87ΔEGFR cells (10^5 cells), anesthetized mice were stereotactically inoculated with 10^5 pfu of HSVQ or RAMBO at the same location. Animals were observed daily and were euthanized at the indicated time points or when they showed signs of morbidity.

For subcutaneous studies, glioma cells (either U87ΔEGFR-Luc (1.5×10^6) o r Gli36ΔEGFR-H2B-RFP (10^6 cells) were implanted subcutaneously into the rear flank of mice. Mice with U87ΔEGFR-Luc tumors were treated six days post tumor implantation (average tumor volume 77–177mm^3) with 8×10^5pfu of RAMBO or HSVQ. Fluorescent molecular tomography (FMT) was performed to assess changes in tumor vascular volume fraction[49]. Briefly mice were injected intravenously with 2 nmoles of a vascular imaging agent (AngioSense680, VisEn Medical, Bedford MA). 15min after probe injection, mice underwent FMT imaging using a commercial FMT imaging system (FMT2500, VisEn Medical). The system generates a 3-dimensional quantitative map of fluorescence by utilizing a Born forward model. Data generated was expressed as local fluorochrome concentration (mean fluorescence within the selected volume).

Mice bearing Gli36ΔEGFR-H2B-RFP tumors (150–250mm^3) received injections of 1×10^6 pfu of RAMBO or HSVQ diluted in HBSS on days 0, 6, 9, and 12. Measurements of tumor volumes were taken as indicated and mice were sacrificed when tumor volumes exceeded 2000mm^3 or greater than 20% of body mass was lost. Mice with a tumor growth of more than 20% from the termination of treatment (day 12) were deemed to have progressed. Mice with a 20% reduction in tumor volume after last treatment were considered to be responders; mice whose tumors remained within 20% after the treatment were deemed to have stable disease.

Immuno Histological analysis

Tumors were fixed in 4% buffered paraformaldehyde followed by 30% sucrose at 4°C then embedded in O.C.T. and frozen at −80°C. Each tumor section was randomly divided into 2–4 pieces and (10μm) sections from each piece were stained with mouse anti-CD31 (Pharmingen, San Jose, CA) to visualize endothelial cells lining the blood vessels (n=3 mice/group). The three most vascularized areas within the tumor ('hot spots') were chosen at low magnification and vessels were counted in a representative high magnification (200×) field in each view field [50]. Single immunoreactive endothelial cells, or endothelial cell clusters separate from other microvessels, were counted as individual microvessels. Mean microvessel density (MVD) was calculated as the average of the counts/view field. Vessels at the periphery of the tumor were disregarded in the MVD counts. The MVD for each therapy group were then averaged together (2–4 sections/tumor, and n=4tumors/group) to get the final count±SEM.

In vitro endothelial cell assays

U251T2 glioma cells were infected with HSVQ or RAMBO (MOI 2) at 4°C for 30 minutes. After 14 hours CM was harvested, cellular debris was removed by centrifugation and free floating viral particles were removed by further centrifugation at 27,700g for 1hr. The CM was then concentrated 100 fold in Amicon-Ultra-centrifuge tubes (Billerica, MA).

For the endothelial cell migration assays, HDMECs cultured in 0.5% serum-containing media overnight were pretreated with concentrated CM for 30 min. 10^6 cells were plated in the upper chamber of Transwell chambers (ISC BioExpress, Kaysville, UT) with an 8μm pore size and complete HDMEC media was used as a chemo-attractant in the bottom chamber. The cells were allowed to migrate for 6hrs, and were then fixed and stained with 0.5%crystal violet. The migrated cells were quantified as number of cells/view-field (N=3 viewfields/filter, and 6 filters/group). For the tube formation assay 40,000 HDMECs cultured as above were plated on 250μL of matrigel (BD Biosciences, Bedford, MA) diluted to 75% concentration in complete HDMEC medium, and incubated at 37°C for 7hrs. Pictures of the formed tubes (200μm or larger and connected at both ends) were quantified by counting one 10x microscopic view/well and the data presented as means of 4 wells.

Statistical Analysis

Students t-test was used to analyze changes in cell killing, HDMEC transwell migration, and tube formation assay data, differences in amount of hemoglobin in DIVAA assay, changes in microvessel density and FMT analysis. A *P* value less than 0.05 was considered statistically significant in Student's *t* test. Kaplan–Meier curves were compared using the log-rank test. All statistical analyses were performed with the use of SPSS statistical software (version 14.0; SPSS Inc, Chicago, IL).

Supplementary Material

Refer to Web version on PubMed Central for supplementary material.

Acknowledgments

Financial Support:

This work was supported by funding from the National Institutes of Health Grant (1K01NS059575; R01NS064607; R21NS056203 to BK; P01 CA069246 to EAC and RW; R24 CA92782 to RW); American Association for Neurological Surgeons/Congress of Neurological Surgeons, Section on Tumors/Brain Lab International Research Fellowship (to KK.); American Brain Tumor Association Medical student summer fellowship (to SA); and The Alex Lemonade Stand Foundation young investigator award (to BK).

REFERENCES

1. Stupp R, Mason WP, van den Bent MJ, Weller M, Fisher B, Taphoorn MJ, Belanger K, Brandes AA, Marosi C, Bogdahn U, Curschmann J, Janzer RC, Ludwin SK, Gorlia T, Allgeier A, Lacombe D, Cairncross JG, Eisenhauer E, Mirimanoff RO. Radiotherapy plus concomitant and adjuvant temozolomide for glioblastoma. N Engl J Med 2005;352:987–996. [PubMed: 15758009]
2. Narayana A, Kelly P, Golfinos J, Parker E, Johnson G, Knopp E, Zagzag D, Fischer I, Raza S, Medabalmi P, Eagan P, Gruber ML. Antiangiogenic therapy using bevacizumab in recurrent high-grade glioma: impact on local control and patient survival. J Neurosurg. 2008
3. Shah AC, Benos D, Gillespie GY, Markert JM. Oncolytic viruses: clinical applications as vectors for the treatment of malignant gliomas. J Neurooncol 2003;65:203–226. [PubMed: 14682372]
4. Liu TC, Galanis E, Kirn D. Clinical trial results with oncolytic virotherapy: a century of promise, a decade of progress. Nat Clin Pract Oncol 2007;4:101–117. [PubMed: 17259931]
5. Haseley A, Christopher A, Chaudhary A, Kaur B. Advances in Oncolytic virus therapy for glioma. Recent Patents on CNS Drug Discovery 2009;4:1–13. [PubMed: 19149710]
6. Choudhary A, Hiscott P, Hart CA, Kaye SB, Batterbury M, Grierson I. Suppression of thrombospondin 1 and 2 production by herpes simplex virus 1 infection in cultured keratocytes. Mol Vis 2005;11:163–168. [PubMed: 15761388]
7. Lee S, Zheng M, Kim B, Rouse BT. Role of matrix metalloproteinase-9 in angiogenesis caused by ocular infection with herpes simplex virus. J Clin Invest 2002;110:1105–1111. [PubMed: 12393846]

8. Leibovich SJ, Polverini PJ, Fong TW, Harlow LA, Koch AE. Production of angiogenic activity by human monocytes requires an L-arginine/nitric oxide-synthase-dependent effector mechanism. Proc Natl Acad Sci U S A 1994;91:4190–4194. [PubMed: 7514298]
9. Zheng M, Deshpande S, Lee S, Ferrara N, Rouse BT. Contribution of vascular endothelial growth factor in the neovascularization process during the pathogenesis of herpetic stromal keratitis. J Virol 2001;75:9828–9835. [PubMed: 11559816]
10. Biswas PS, Rouse BT. Early events in HSV keratitis--setting the stage for a blinding disease. Microbes Infect 2005;7:799–810. [PubMed: 15857807]
11. Aghi M, Rabkin SD, Martuza RL. Angiogenic response caused by oncolytic herpes simplex virus-induced reduced thrombospondin expression can be prevented by specific viral mutations or by administering a thrombospondin-derived peptide. Cancer Res 2007;67:440–444. [PubMed: 17234749]
12. Kurozumi K, Hardcastle J, Thakur R, Shroll J, Nowicki M, Otsuki A, Chiocca EA, Kaur B. Oncolytic HSV-1 infection of tumors induces angiogenesis and upregulates CYR61. Mol Ther 2008;16:1382–1391. [PubMed: 18545226]
13. Grote K, Salguero G, Ballmaier M, Dangers M, Drexler H, Schieffer B. The angiogenic factor CCN1 promotes adhesion and migration of circulating CD34+ progenitor cells: potential role in angiogenesis and endothelial regeneration. Blood 2007;110:877–885. [PubMed: 17429007]
14. de Fraipont F, Nicholson AC, Feige JJ, Van Meir EG. Thrombospondins and tumor angiogenesis. Trends Mol Med 2001;7:401–407. [PubMed: 11530335]
15. Kaur B, Brat DJ, Devi NS, Van Meir EG. Vasculostatin, a proteolytic fragment of brain angiogenesis inhibitor 1, is an antiangiogenic and antitumorigenic factor. Oncogene 2005;24:3632–3642. [PubMed: 15782143]
16. Babic AM, Kireeva ML, Kolesnikova TV, Lau LF. CYR61, a product of a growth factor-inducible immediate early gene, promotes angiogenesis and tumor growth. Proc Natl Acad Sci U S A 1998;95:6355–6360. [PubMed: 9600969]
17. Monnier Y, Farmer P, Bieler G, Imaizumi N, Sengstag T, Alghisi GC, Stehle JC, Ciarloni L, Andrejevic-Blant S, Moeckli R, Mirimanoff RO, Goodman SL, Delorenzi M, Ruegg C. CYR61 and alphaVbeta5 integrin cooperate to promote invasion and metastasis of tumors growing in preirradiated stroma. Cancer Res 2008;68:7323–7331. [PubMed: 18794119]
18. Koh JT, Kook H, Kee HJ, Seo YW, Jeong BC, Lee JH, Kim MY, Yoon KC, Jung S, Kim KK. Extracellular fragment of brain-specific angiogenesis inhibitor 1 suppresses endothelial cell proliferation by blocking alphavbeta5 integrin. Exp Cell Res 2004;294:172–184. [PubMed: 14980512]
19. Nishimori H, Shiratsuchi T, Urano T, Kimura Y, Kiyono K, Tatsumi K, Yoshida S, Ono M, Kuwano M, Nakamura Y, Tokino T. A novel brain-specific p53-target gene, BAI1, containing thrombospondin type 1 repeats inhibits experimental angiogenesis. Oncogene 1997;15:2145–2150. [PubMed: 9393972]
20. Kaur B, Cork SM, Sandberg E, Devi NS, Zhang Z, Klenotic PA, Febbraio M, Shim H, Mao H, Tucker-Burder C, Silverstein RL, Brat DJ, Olson JJ, Van Meir EG. Vasculostatin, a 120kDa BAI1 fragment can efficiently inhibit intracranial angiogenesis and tumorigenesis, despite a proangiogenic stimulus. Cancer Research. 2009 In Press.
21. Mullen JT, Donahue JM, Chandrasekhar S, Yoon SS, Liu W, Ellis LM, Nakamura H, Kasuya H, Pawlik TM, Tanabe KK. Oncolysis by viral replication and inhibition of angiogenesis by a replication-conditional herpes simplex virus that expresses mouse endostatin. Cancer 2004;101:869–877. [PubMed: 15305421]
22. Liu TC, Zhang T, Fukuhara H, Kuroda T, Todo T, Canron X, Bikfalvi A, Martuza RL, Kurtz A, Rabkin SD. Dominant-negative fibroblast growth factor receptor expression enhances antitumoral potency of oncolytic herpes simplex virus in neural tumors. Clin Cancer Res 2006;12:6791–6799. [PubMed: 17121900]
23. Liu TC, Zhang T, Fukuhara H, Kuroda T, Todo T, Martuza RL, Rabkin SD, Kurtz A. Oncolytic HSV Armed with Platelet Factor 4, an Antiangiogenic Agent, Shows Enhanced Efficacy. Mol Ther 2006;14:789–797. [PubMed: 17045531]

24. Bonnefoy A, Moura R, Hoylaerts MF. The evolving role of thrombospondin-1 in hemostasis and vascular biology. Cell Mol Life Sci 2008;65:713–727. [PubMed: 18193161]
25. Mahller YY, Vaikunth SS, Ripberger MC, Baird WH, Saeki Y, Cancelas JA, Crombleholme TM, Cripe TP. Tissue inhibitor of metalloproteinase-3 via oncolytic herpesvirus inhibits tumor growth and vascular progenitors. Cancer Res 2008;68:1170–1179. [PubMed: 18281493]
26. Terada K, Wakimoto H, Tyminski E, Chiocca EA, Saeki Y. Development of a rapid method to generate multiple oncolytic HSV vectors and their in vivo evaluation using syngeneic mouse tumor models. Gene Ther 2006;13:705–714. [PubMed: 16421599]
27. Sundaresan P, Hunter WD, Martuza RL, Rabkin SD. Attenuated, replication-competent herpes simplex virus type 1 mutant G207: safety evaluation in mice. J Virol 2000;74:3832–3841. [PubMed: 10729157]
28. Todo T, Feigenbaum F, Rabkin SD, Lakeman F, Newsome JT, Johnson PA, Mitchell E, Belliveau D, Ostrove JM, Martuza RL. Viral shedding and biodistribution of G207, a multimutated, conditionally replicating herpes simplex virus type 1, after intracerebral inoculation in aotus. Mol Ther 2000;2:588–595. [PubMed: 11124059]
29. Markert JM, Liechty PG, Wang W, Gaston S, Braz E, Karrasch M, Nabors LB, Markiewicz M, Lakeman AD, Palmer CA, Parker JN, Whitley RJ, Gillespie GY. Phase Ib Trial of Mutant Herpes Simplex Virus G207 Inoculated Pre-and Post-tumor Resection for Recurrent GBM. Mol Ther 2009;17:8–9. [PubMed: 19116635]
30. Kaur B, Brat DJ, Calkins CC, Van Meir EG. Brain angiogenesis inhibitor 1 is differentially expressed in normal brain and glioblastoma independently of p53 expression. Am J Pathol 2003;162:19–27. [PubMed: 12507886]
31. de Visser KE, Eichten A, Coussens LM. Paradoxical roles of the immune system during cancer development. Nat Rev Cancer 2006;6:24–37. [PubMed: 16397525]
32. Kurozumi K, Hardcastle J, Thakur R, Yang M, Christoforidis G, Fulci G, Hochberg FH, Weissleder R, Carson W, Chiocca EA, Kaur B. Effect of tumor microenvironment modulation on the efficacy of oncolytic virus therapy. J Natl Cancer Inst 2007;99:1768–1781. [PubMed: 18042934]
33. Fulci G, Dmitrieva N, Gianni D, Fontana EJ, Pan X, Lu Y, Kaufman CS, Kaur B, Lawler SE, Lee RJ, Marsh CB, Brat DJ, van Rooijen N, Stemmer-Rachamimov AO, Hochberg FH, Weissleder R, Martuza RL, Chiocca EA. Depletion of peripheral macrophages and brain microglia increases brain tumor titers of oncolytic viruses. Cancer Res 2007;67:9398–9406. [PubMed: 17909049]
34. Fulci G, Breymann L, Gianni D, Kurozomi K, Rhee SS, Yu J, Kaur B, Louis DN, Weissleder R, Caligiuri MA, Chiocca EA. Cyclophosphamide enhances glioma virotherapy by inhibiting innate immune responses. Proc Natl Acad Sci U S A 2006;103:12873–12878. [PubMed: 16908838]
35. Kunstfeld R, Hirakawa S, Hong YK, Schacht V, Lange-Asschenfeldt B, Velasco P, Lin C, Fiebiger E, Wei X, Wu Y, Hicklin D, Bohlen P, Detmar M. Induction of cutaneous delayed-type hypersensitivity reactions in VEGF-A transgenic mice results in chronic skin inflammation associated with persistent lymphatic hyperplasia. Blood 2004;104:1048–1057. [PubMed: 15100155]
36. Oura H, Bertoncini J, Velasco P, Brown LF, Carmeliet P, Detmar M. A critical role of placental growth factor in the induction of inflammation and edema formation. Blood 2003;101:560–567. [PubMed: 12393422]
37. Libertini S, Iacuzzo I, Perruolo G, Scala S, Ierano C, Franco R, Hallden G, Portella G. Bevacizumab increases viral distribution in human anaplastic thyroid carcinoma xenografts and enhances the effects of E1A-defective adenovirus dl922-947. Clin Cancer Res 2008;14:6505–6514. [PubMed: 18927290]
38. Zohrabian VM, Nandu H, Gulati N, Khitrov G, Zhao C, Mohan A, Demattia J, Braun A, Das K, Murali R, Jhanwar-Uniyal M. Gene expression profiling of metastatic brain cancer. Oncol Rep 2007;18:321–328. [PubMed: 17611651]
39. Hatanaka H, Oshika Y, Abe Y, Yoshida Y, Hashimoto T, Handa A, Kijima H, Yamazaki H, Inoue H, Ueyama Y, Nakamura M. Vascularization is decreased in pulmonary adenocarcinoma expressing brain-specific angiogenesis inhibitor 1 (BAI1). Int J Mol Med 2000;5:181–183. [PubMed: 10639598]
40. Nam DH, Park K, Suh YL, Kim JH. Expression of VEGF and brain specific angiogenesis inhibitor-1 in glioblastoma: prognostic significance. Oncol Rep 2004;11:863–869. [PubMed: 15010886]

41. Lee JH, Koh JT, Shin BA, Ahn KY, Roh JH, Kim YJ, Kim KK. Comparative study of angiostatic and anti-invasive gene expressions as prognostic factors in gastric cancer. Int J Oncol 2001;18:355–361. [PubMed: 11172604]

42. Fukushima Y, Oshika Y, Tsuchida T, Tokunaga T, Hatanaka H, Kijima H, Yamazaki H, Ueyama Y, Tamaoki N, Nakamura M. Brain-specific angiogenesis inhibitor 1 expression is inversely correlated with vascularity and distant metastasis of colorectal cancer. Int J Oncol 1998;13:967–970. [PubMed: 9772287]

43. Kang X, Xiao X, Harata M, Bai Y, Nakazaki Y, Soda Y, Kurita R, Tanaka T, Komine F, Izawa K, Kunisaki R, Setoyama M, Nishimori H, Natsume A, Sunamura M, Lozonshi L, Saitoh I, Tokino T, Asano S, Nakamura Y, Tani K. Antiangiogenic activity of BAI1 in vivo: implications for gene therapy of human glioblastomas. Cancer Gene Ther 2006;13:385–392. [PubMed: 16244591]

44. Kudo S, Konda R, Obara W, Kudo D, Tani K, Nakamura Y, Fujioka T. Inhibition of tumor growth through suppression of angiogenesis by brain-specific angiogenesis inhibitor 1 gene transfer in murine renal cell carcinoma. Oncol Rep 2007;18:785–791. [PubMed: 17786337]

45. Park D, Tosello-Trampont AC, Elliott MR, Lu M, Haney LB, Ma Z, Klibanov AL, Mandell JW, Ravichandran KS. BAI1 is an engulfment receptor for apoptotic cells upstream of the ELMO/Dock180/Rac module. Nature. 2007

46. Kambara H, Okano H, Chiocca EA, Saeki Y. An oncolytic HSV-1 mutant expressing ICP34.5 under control of a nestin promoter increases survival of animals even when symptomatic from a brain tumor. Cancer Res 2005;65:2832–2839. [PubMed: 15805284]

47. Hudziak RM, Lewis GD, Winget M, Fendly BM, Shepard HM, Ullrich A. p185HER2 monoclonal antibody has antiproliferative effects in vitro and sensitizes human breast tumor cells to tumor necrosis factor. Mol Cell Biol 1989;9:1165–1172. [PubMed: 2566907]

48. Markert JM, Medlock MD, Rabkin SD, Gillespie GY, Todo T, Hunter WD, Palmer CA, Feigenbaum F, Tornatore C, Tufaro F, Martuza RL. Conditionally replicating herpes simplex virus mutant, G207 for the treatment of malignant glioma: results of a phase I trial. Gene Ther 2000;7:867–874. [PubMed: 10845725]

49. Montet X, Figueiredo JL, Alencar H, Ntziachristos V, Mahmood U, Weissleder R. Tomographic fluorescence imaging of tumor vascular volume in mice. Radiology 2007;242:751–758. [PubMed: 17325064]

50. Choi WW, Lewis MM, Lawson D, Yin-Goen Q, Birdsong GG, Cotsonis GA, Cohen C, Young AN. Angiogenic and lymphangiogenic microvessel density in breast carcinoma: correlation with clinicopathologic parameters and VEGF-family gene expression. Mod Pathol 2005;18:143–152. [PubMed: 15297858]

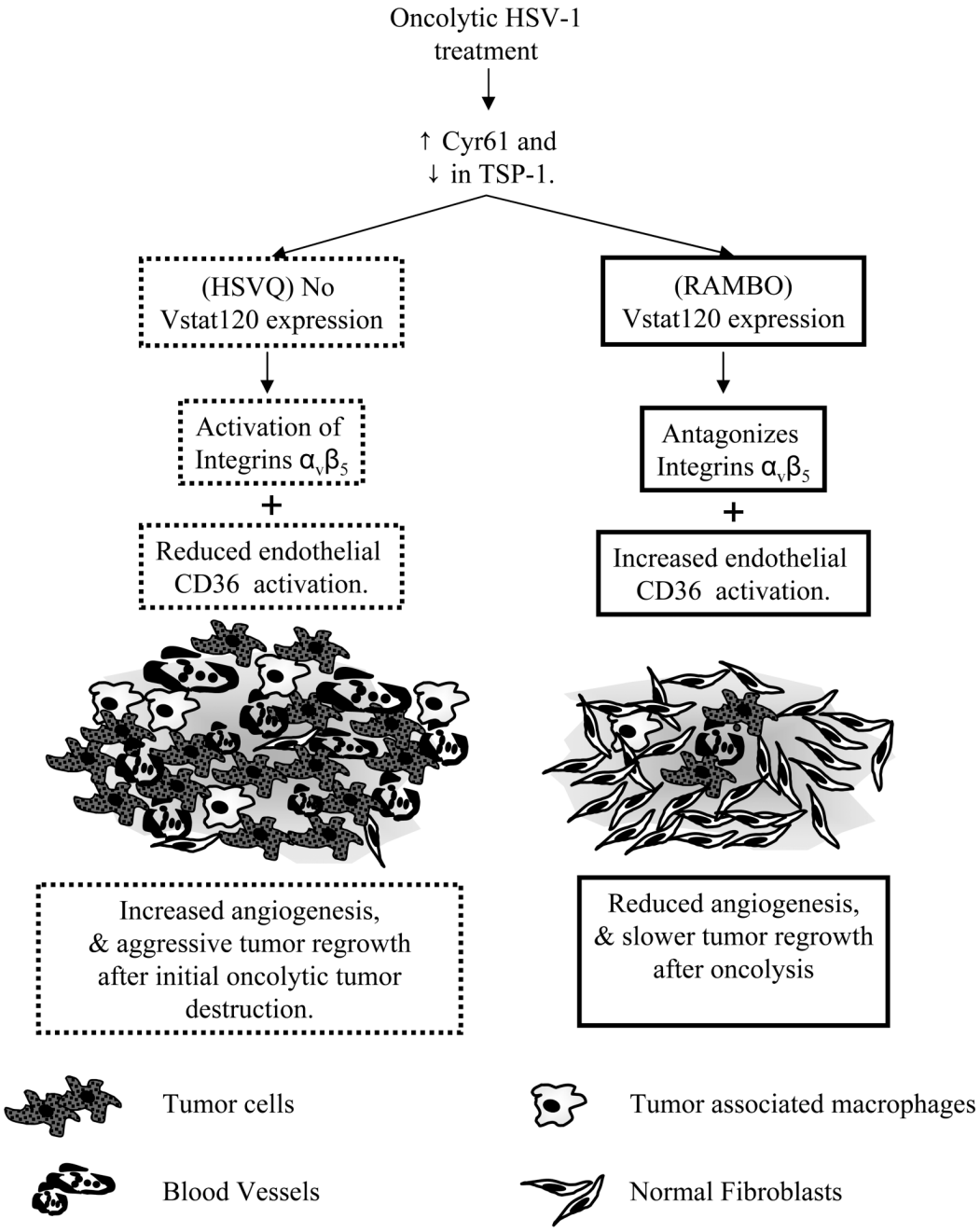

Figure 1. Rationale for the construction of Vstat120 expressing OV

Increased Cyr61 and reduced TSP-1 expression in the tumor microenvironment upon OV treatment. Increased Cyr61 would lead to integrin mediated activation of endothelial cells resulting in angiogenesis. Reduction in antiangiogenic TSP-1 would further tilt the scale toward increased angiogenesis. Vstat120 expression by RAMBO would counter both of these effects and inhibit angiogenesis of the residual disease.

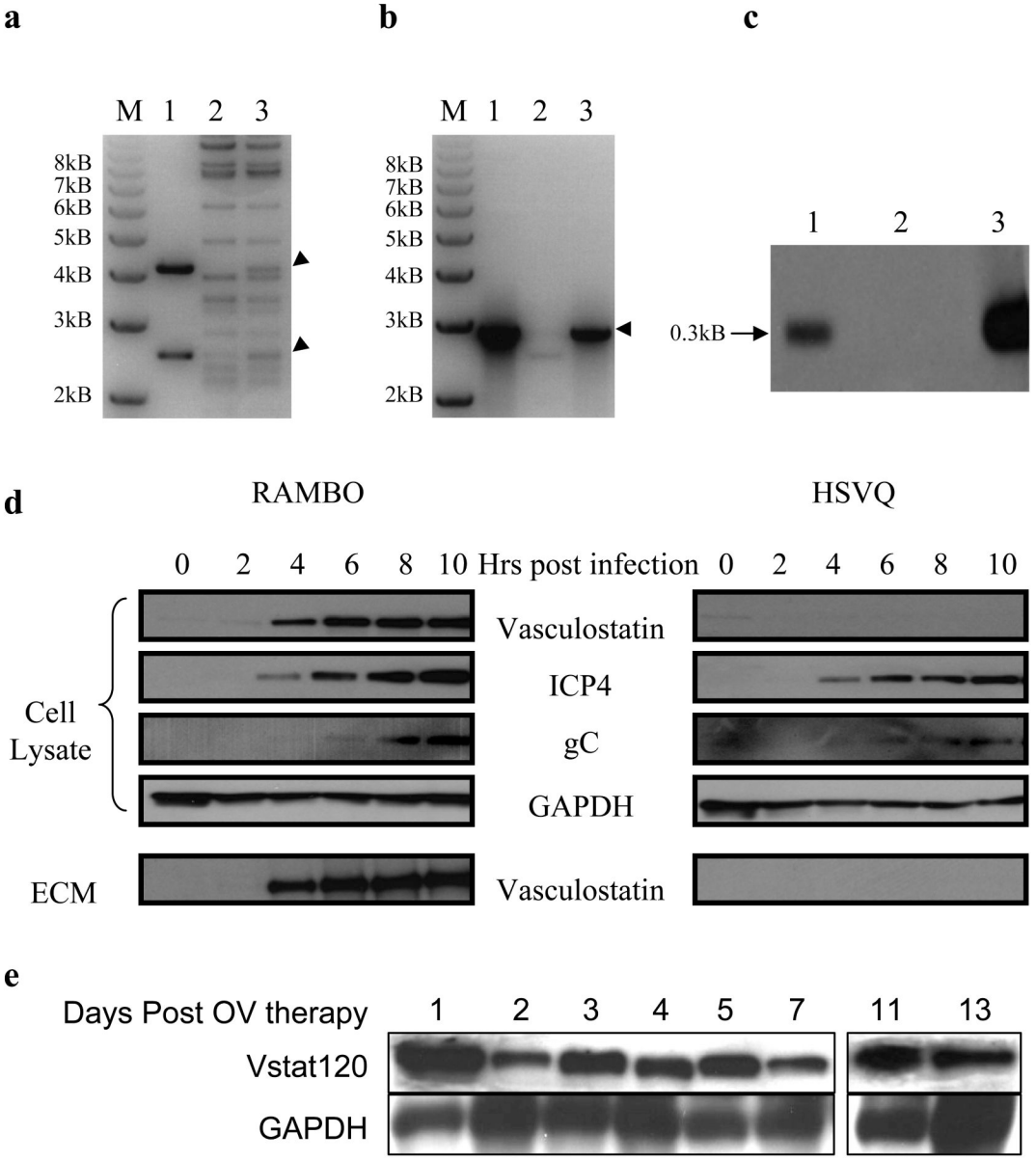

Figure 2. Verification of RAMBO and Vstat120 production *in vitro* and *in vivo*

(a) XhoI Restriction Digest of pVasculo-transfer plasmid expressing IE4/5 promotor-Vstat120 cassette (lane 1) control fHSVQ1-BAC (lane 2) and RAMBO-BAC (lane 3). The expected 4.2kb, and 2.5kb restriction fragments are indicated by arrow heads. (**b)** PCR of recombinant RAMBO-BAC. DNA from control plasmid pVasculo-transfer (lane 1), fHSVQ1 (lane 2), or RAMBO-BAC (Lane 3) was used as a template to detect the presence of Vstat120 gene by PCR using Vstat120 specific primers. (**c)** Southern blot analysis of HSVQ and RAMBO viral isolates digested with *XhoI*, and probed for a Vstat120 specific fragments. Hybridization of the expected 0.3 kb fragment to *XhoI*-digested DNA in RAMBO (lane 1) and pVasculo-transfer (lane 3) but not in HSVQ (lane 2) digeted lanes is indicated by an arrow. **(d)** Immunoblot of LN229 glioma cells infected with RAMBO or HSVQ at an MOI = 0.05. The cell lysate and ECM were harvested at 0, 2, 4, 6, 8, and 10 hours after infection as described in materials and methods. Temporal pattern of expression of Vstat120 was investigated by western blot analysis

of the cell lysate and ECM. Note that the production of Vstat120 coincides with the turning on of the immediate early viral ICP4 gene. **(e)** Immunoblot of Vstat120 propagation in subcutaneous gliomas (U87ΔEGFR-Luc) treated with RAMBO *in vivo* over time. Mice with subcutaneous tumors were treated with a single intratumoral injection of RAMBO (8×10^5 pfu) and the mice were sacrificed on days 1, 2, 3, 4, 5, 7, 11 and 13 following therapy. The harvested tumor was lysed and analyzed for expression of Vstat120 by western blot analysis. Note the detectable presence of Vstat120 within the tumor even 13 days post OV therapy.

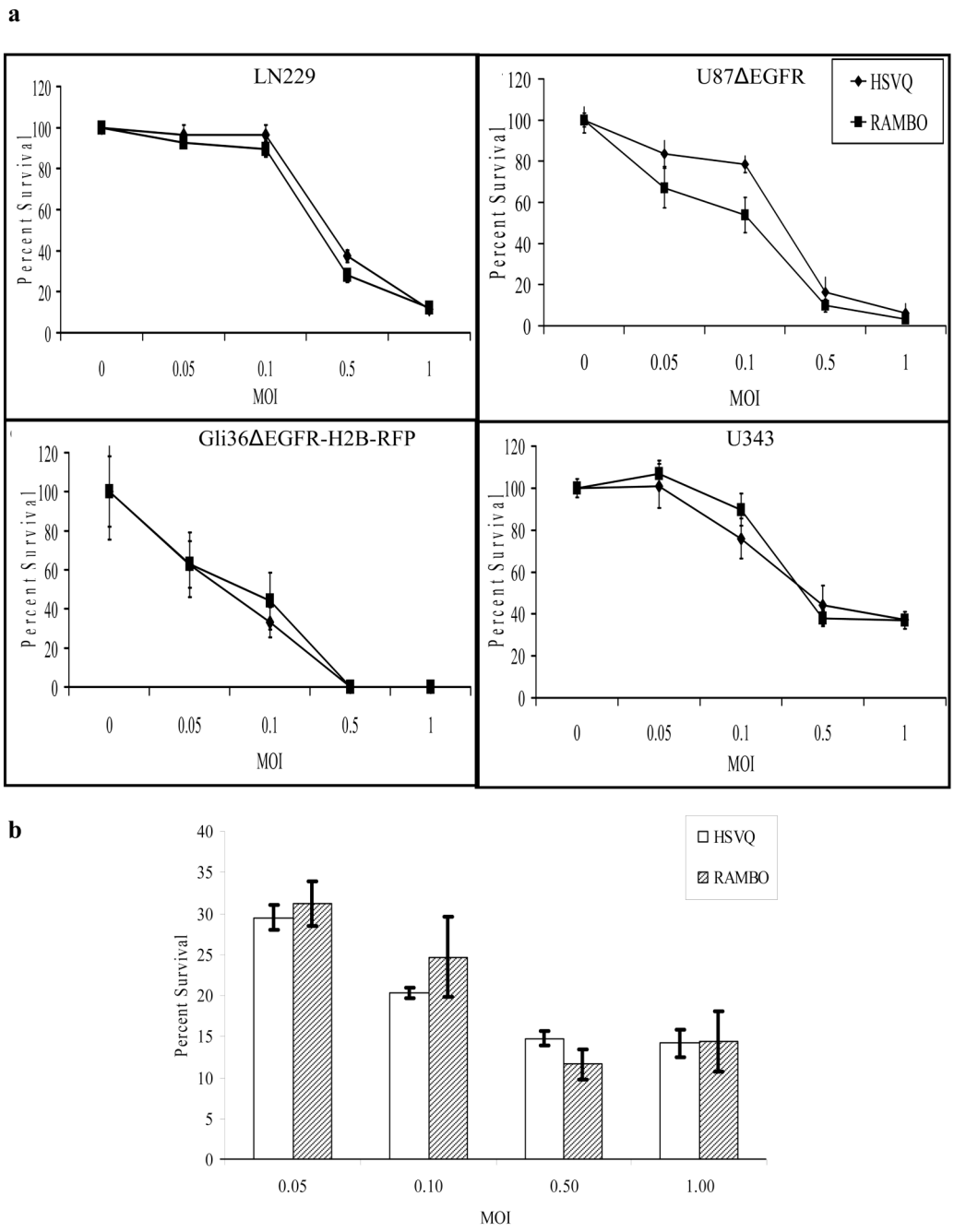

Figure 3. Cytotoxicity of RAMBO and HSVQ towards glioma cell lines and Normal human astrocytes

(a) The *in vitro* cytotoxicity of RAMBO was compared to HSVQ in LN229, U87ΔEGFR, Gli36ΔEGFR-H2B-RFP and U343 cells. The percentage of viable cells relative to uninfected cells was measured by crystal violet assay on day three. **(b)** Cytotoxicity of RAMBO and HSVQ towards Normal Human Astrocytes (NHA). NHA cells were infected with HSVQ or RAMBO at the indicated MOIs. Seventy-two hours later the percent survival was assessed by a standard colorimetric crystal violet assay. Data shown are the mean ± SD % survival relative to uninfected cells. Note no significant difference in the number of viable cells infected with HSVQ or RAMBO at each MOI.

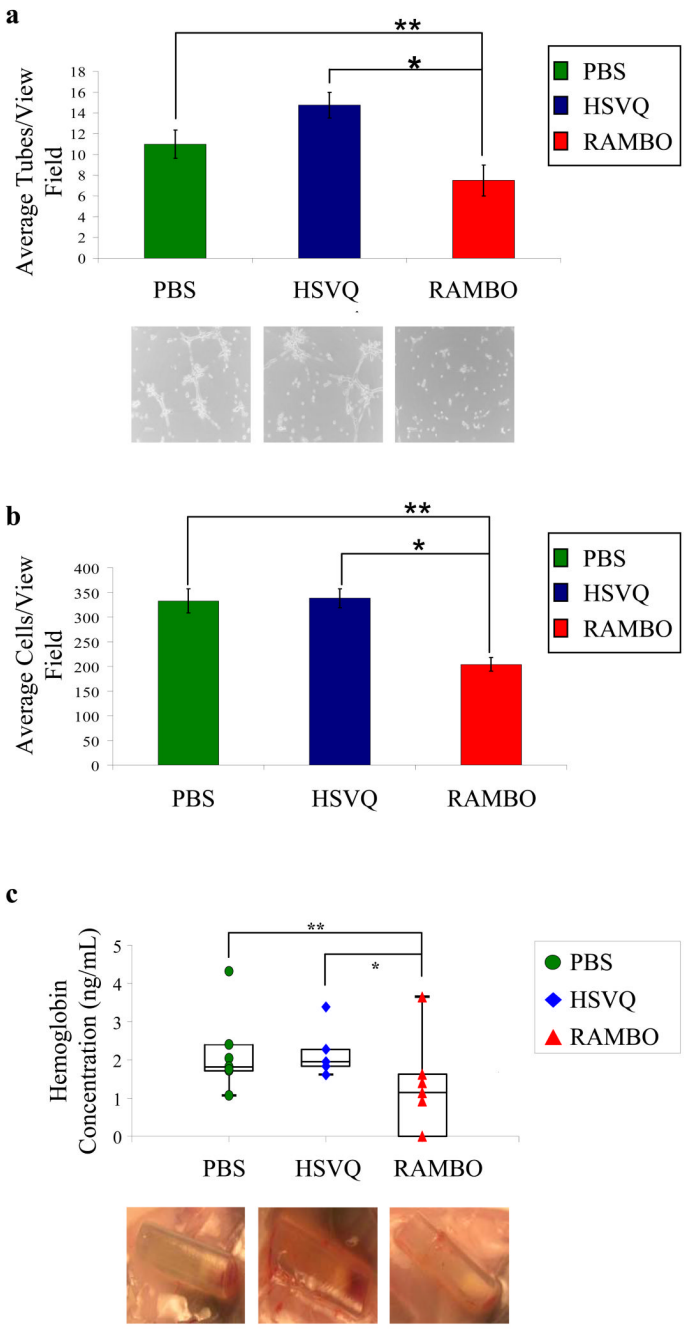

Figure 4. Antiangiogenic Effect of RAMBO

(a) Inhibition of endothelial cell tube formation: HDMEC's were incubated with CM derived from U251T2 cells treated with PBS, HSVQ, or RAMBO. The cells were then plated on matrigel and HDMEC's were allowed to form tubes for six hours. The number of tubes >200μm were quantified (n=4/group). Data are presented as mean ± SEM of number of tubes/view field. The bottom panel shows representative images of tube formation. Note the statistically significant reduction in tube formation of HDMEC's incubated with CM from RAMBO treated cells compared to PBS (**) or HSVQ (*) treated cells respectively (***P*=0.0273, and **P*=0.0184 respectively). **(b)** Inhibition of endothelial cell migration: HDMECs were incubated with CM derived from U251T2 cells treated with PBS, HSVQ, or RAMBO. The

cells were plated in the upper chamber of transwell chambers and allowed to migrate towards complete HDMEC media used as a chemo-attractant in the bottom chamber. The migrated cells on the bottom side of the filter were quantified as described (n=14, 15 and 16 view fields for PBS, HSVQ and RAMBO respectively). Data are presented as mean ± SEM of number of cells/view field. Note the statistically significant reduction in migration of HDMEC's incubated with CM from RAMBO treated cells compared to PBS (**) or HSVQ (*) treated cells respectively (**P=0.0004, and *P=0.0005 respectively). **(c)** *In vivo* inhibition of angiogenesis upon RAMBO infection of glioma cells: The antiangiogenic capabilities of RAMBO were tested using the Trevigen Direct *in Vivo* Angiogenesis Assay (DIVAA) kit. Angioreactors filled with U87ΔEGFR cells treated with PBS HSVQ, or RAMBO were mixed with basement membrane and implanted subcutaneously into the rear flanks of nu/nu mice. Eleven days later the mice were sacrificed and the angioreactors removed. The amount of angiogenesis that occurred in the angioreactors was quantified using the Wako Hemoglobin B kit. Data shown are the mean ± SEM amount of hemoglobin in the tubes. Note both visually and graphically the significant reduction in angiogenesis for samples infected with RAMBO compared to HSVQ (n=7/group, and P=0.007) and PBS control (P=0.0022).

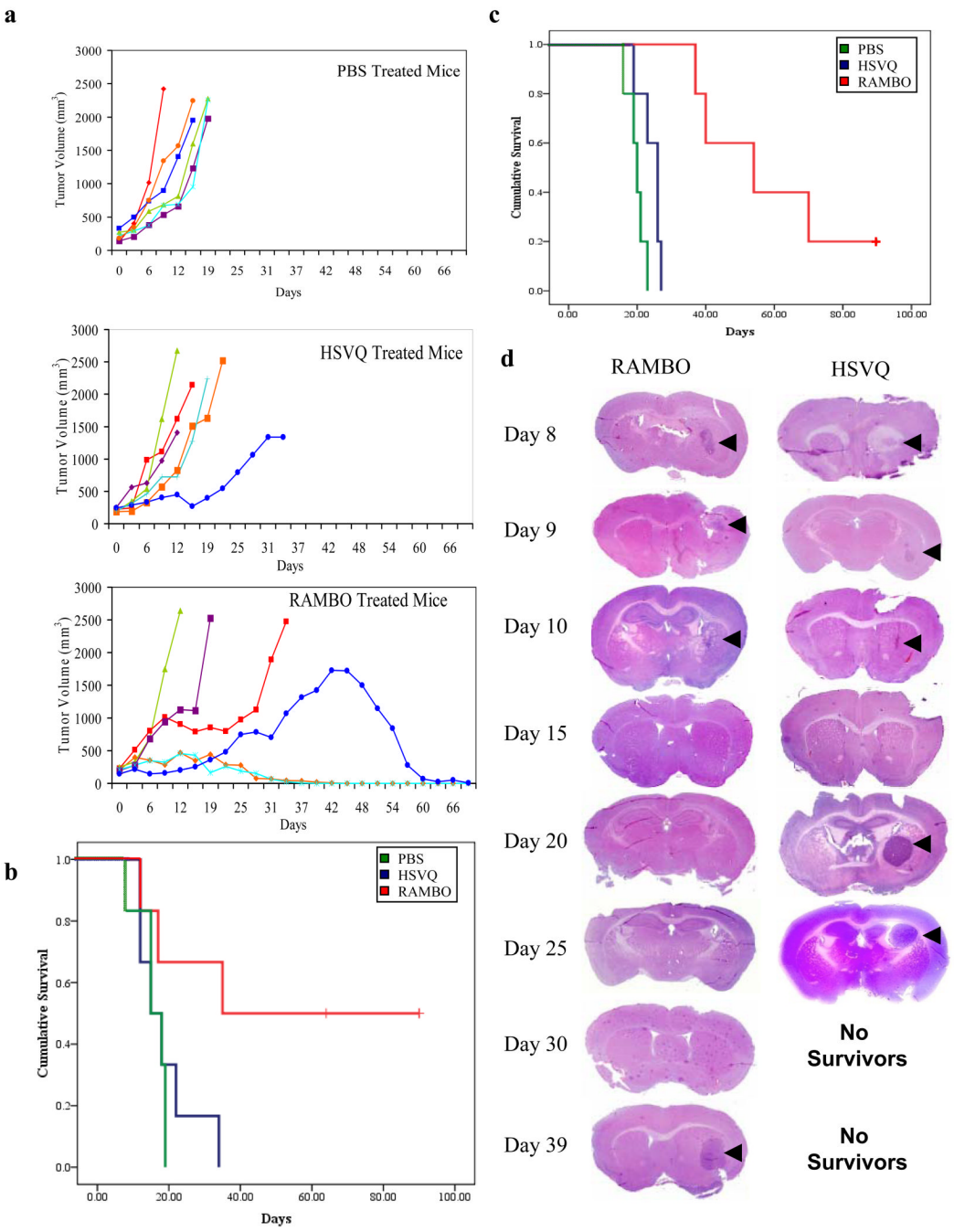

Figure 5. Increased Anti tumor efficacy of RAMBO compared to HSVQ

(a) Antitumor efficacy of RAMBO against subcutaneous Gli36ΔEGFR-H2B-RFP. Mice with subcutaneous Gli36ΔEGFR-H2B-RFP tumors (Range= 150–250 mm^3) were treated with PBS or 1×10^6 p.f.u of HSVQ or RAMBO on days 0, 6, 9, and 12 (n=6/group) by direct intratumoral injection. Mice were closely monitored for tumor growth, and were euthanized when their tumors reached 2000 mm^3, or when they lost more than 20% of body weight. The tumor growth of individual mice treated with PBS (Top Panel), HSVQ (middle panel), and RAMBO (bottom panel) is shown as a function of time. **(b)** Kaplan-Meier survival curve of mice with subcutaneous Gli36ΔEGFR-H2B-RFP tumors treated with PBS, HSVQ or RAMBO. Mice treated with RAMBO showed a significant improvement in their survival compared to mice

treated with HSVQ (P=0.038). **(c)** Kaplan-Meier survival curve of mice implanted with intracranial U87ΔEGFR glioma treated with PBS, HSVQ or RAMBO. Briefly, athymic nude mice bearing intracranial U78ΔEGFR gliomas were treated with PBS or 1×10^5 pfu of HSVQ or RAMBO seven days post tumor cell implantation. The mice were then closely monitored for survival. Note the statistically significant improvement in median survival of mice treated with RAMBO compared to HSVQ treated mice (P=0.002). **(d)** In a separate intracranial glioma experiment (same as outlined in 5C) mice were treated with HSVQ or RAMBO and sacrificed on the days indicated post-OV therapy. The harvested brains were then fixed and sectioned for H&E. Shown are representative images of the H&E sections indicating the reduction in tumor size (arrows) after treatment with HSVQ or RAMBO. Note the similar rate of tumor regression following OV therapy for RAMBO and HSVQ treated mice and then re-growth of the residual tumor for HSVQ treated mice by day 20, as compared to day 39 for the RAMBO treated mice.

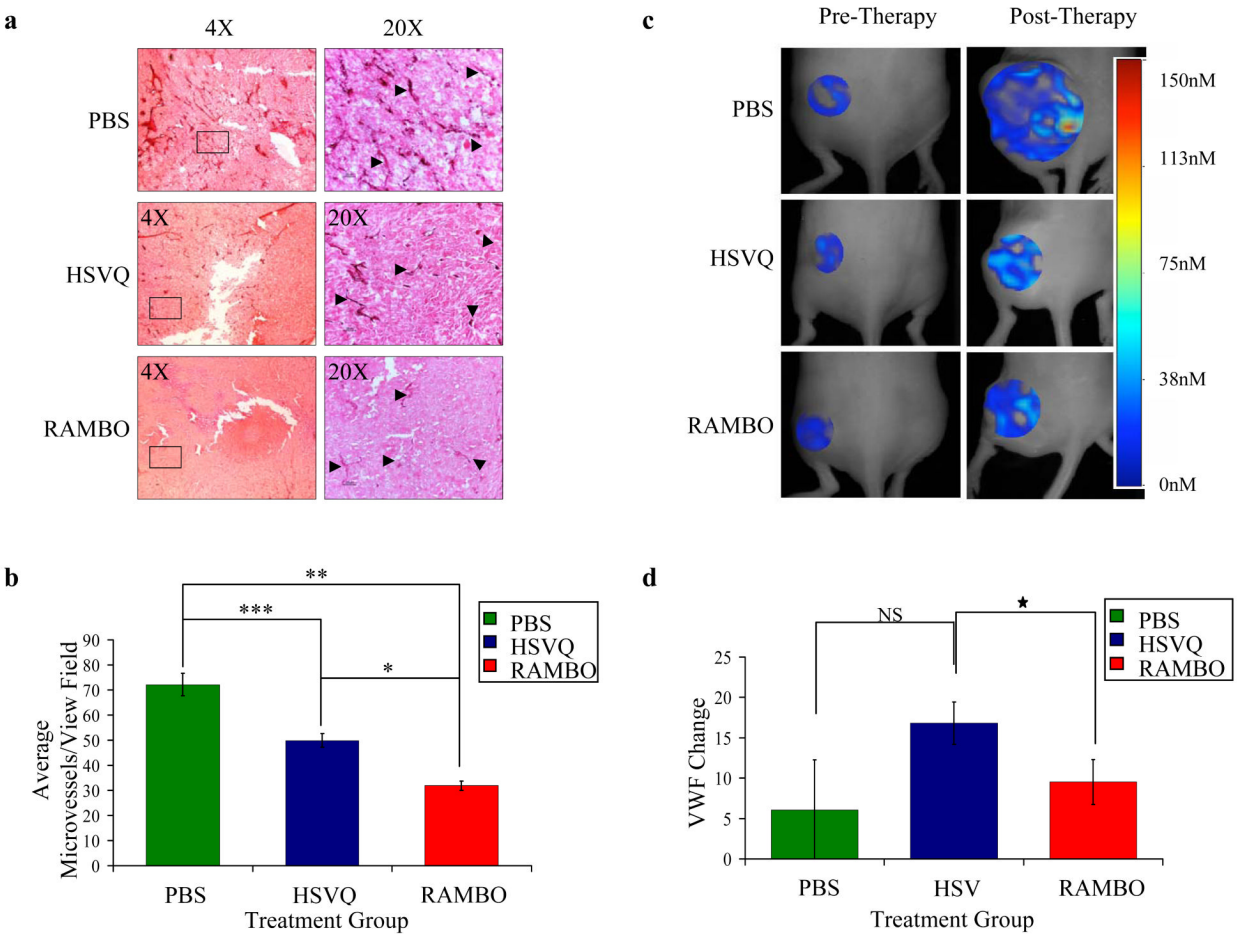

Figure 6. Reduced microvessel density and perfusion in animals treated with RAMBO compared to HSVQ

Mice with subcutaneous U87ΔEGFR-Luc tumors were treated with single dose (8 ×10^5 pfu) of PBS, HSVQ or RAMBO six days post tumor cell implantation. **(a)** Representative pictures of immunohistochemistry for CD31 staining of tumors derived from mice 12 days post therapy with either PBS (Top), HSVQ (Middle), or RAMBO (Bottom). **(b)** Quantification of MVD in tumors treated with PBS, HSVQ or RAMBO. Data shown are mean MVD ± SEM for each group (n=2 to 4 sections/tumor and n=4 tumors/group) Note the significant difference in MVD for RAMBO vs. HSVQ (*p=0.0001), PBS vs. RAMBO (**P=0.0001), and PBS vs. HSVQ (***P=0.0038). In a separate experiment mice bearing established subcutaneous U87ΔEGFR-Luc tumors treated with PBS or HSVQ or RAMBO were compared for vascular perfusion by fluorescent molecular tomography (FMT). Mice were intravenously injected with AngioSense680, and underwent FMT imaging day before (left panel) and twelve days after therapy (right panel). **(c)** Representative images of FMT of mice treated with PBS, HSVQ or RAMBO. Local fluorochrome concentrations were color coded. Shift towards red indicates higher fluorochrome concentration and shift towards blue indicates lower fluorochrome concentration. Higher fluorochrome concentration indicates higher vascular perfusion in that area. The very large size of PBS treated tumors resulted in some areas of very high perfusion (red area representing probe concentrations of 115–150nM) along with large areas of necrosis with poor to no perfusion (no color to blue color representing probe concentrations of 0–38nM). **(d)** Mean VVF change for mice treated with PBS, HSVQ or RAMBO. Relative vascular volume fractions (VVF) were calculated by dividing the total fluorochrome concentration in

each tumor by the corresponding tumor volume. VVF change was calculated by subtracting the pre-therapy VVF for each mice from the post therapy VVF. Data shown are the mean VVF change ± SEM. PBS treated tumors grew aggressively and were large tumors with local hot spots of perfused vessels but largely devoid of perfusion. VVF values for PBS treated tumors thus had a trend to be lower than that for HSVQ and RAMBO. Between the relatively similar sized HSVQ and RAMBO tumors, HSVQ had in general better perfusion (range of about 0–75nM) than RAMBO, (0–38nM). Note the statistically significant reduction in VVF change for the tumors of mice treated with RAMBO compared to HSVQ treated tumors ($P<0.05$) (n=4 and n=3, respectively).